

# Control-relevant Multiple Linear Modeling of Simulated Moving Bed Chromatography

Girish Sharma, S V Vignesh, K Hariprasad, Sharad Bhartiya \*

*Department of Chemical Engineering,  
Indian Institute of Technology-Bombay, Mumbai - 400 076 India*

**Abstract:** In this work, we propose a control-relevant multiple linear modeling approach for simulated moving bed chromatography (SMBC) by linearizing the first principles model at carefully chosen equilibrium points. Subsequently, sub-models to account for port switching for each of the linear model are obtained. Model aggregation is done using Bayesian weighting to generate multiple model predictions for the nonlinear dynamics of SMBC. The multiple model approach is validated using simulations for cyclic steady state (CSS) of SMB as well as for a transition between two optimal CSS points for separation of a glucose- fructose mixture.

**Keywords:** Simulated moving bed chromatography, separation process, cyclic steady state, glucose-fructose system, multiple linear modeling, Bayesian approach

## 1. INTRODUCTION

Model predictive control (MPC) of SMB requires a simple process model which describes the states and captures the dynamics and switching of the inlet and outlet ports. The first principles model of SMBC is typically a nonlinear partial differential equation and its use in MPC will require an online solution of Nonlinear Program (NLP) in a fraction of sampling period, which is computationally demanding (Alamir et al., 2006; Erdem et al., 2004; Klatt et al., 2002). In literature, linear modeling of SMBC has been illustrated by Natarajan and Lee (2000) and Song et al. (2006). An alternate approach consists of using a multiple model strategy based on simpler approximate control-relevant models, which when aggregated capture both the switching behavior as well as nonlinear dynamics and are suitable for model based control. Such control-relevant models could be developed either from the first principles models or directly identified from data. The multiple model approach is based on the “divide and conquer” principle, that decomposes a nonlinear system into several linear models to capture true nonlinear plant dynamics (Du and Johansen, 2014; Murray-Smith and Johansen, 1997; Banerjee et al., 1997; Hariprasad et al., 2012). In the present work, we propose a multiple modeling strategy for SMBC, wherein the separation of a glucose/fructose mixture is carried out. The first principles model of SMBC, which consists of a set of bi-linear Partial Differential Algebraic Equations is converted to an ODE-IVP and linearized at various equilibrium points. These models are further aggregated using a Bayesian weighting approach to obtain a global linear model at each time instant.

The paper is organized as follows: Section 2 presents a brief overview of the SMBC process and a summary of the first principles model from the literature. Section 3 discusses

\* Corresponding Author: bhartiya@che.iitb.ac.in (Sharad Bhartiya), Tel: +91 22 25767225.

generation of a bank of linear models and Bayesian method for aggregation. Simulation results validating the multiple model approach are presented in Section 4. Finally, conclusions are presented in Section 5.

## 2. MATHEMATICAL MODEL OF SMBC

SMBC process consists of multiple adsorbent-laden columns which are connected in series in a circular manner as shown in Fig. 1. Feed and desorbent streams continuously enter the system and the extract and raffinate streams exit out. A counter current movement of the solid bed is approxi-

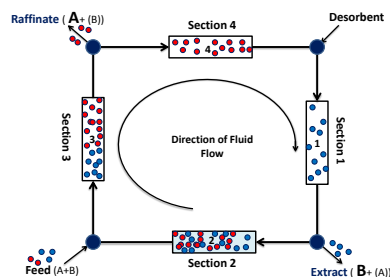


Fig. 1. Schematic of 4 column SMBC unit

mated by sequentially switching the inlet and outlet ports. Four port switches constitute one cycle of SMB operation and after sufficient number of cycles, concentration profiles inside the columns over a cycle become identical to those observed in the previous cycle and a cyclic steady state (CSS) is said to have been reached.

In order to synthesize multiple linear models of the SMB, a first principles dynamic model of the continuous chromatographic process for the separation of glucose/fructose from literature is used. We summarize the model equations here but cite Rajendran et al. (2009); Kawajiri and Biegler (2006) for details.

Let  $c_{ij}$ ,  $q_{ij}$  represent the concentration of the  $i^{th}$  component in the  $j^{th}$  column in the liquid and solid phases respectively,  $v_j$  and  $Q_j$  be the axial velocity and flow rates respectively in the  $j^{th}$  column,  $D_i$  be the dispersion coefficient for  $i^{th}$  species and  $L$  be the length of the column.

Transport Model equations:

$$\frac{\partial c_{ij}}{\partial t} + \frac{(1-\epsilon)}{\epsilon} \frac{dq_{ij}}{dt} = -v_j \frac{\partial c_{ij}}{\partial z} + D_i \frac{\partial^2 c_{ij}}{\partial z^2} \quad (1)$$

$$\frac{\partial q_{ij}}{\partial t} = k_i (q_{ij}^* - q_{ij}); \quad q_{ij}^* = K_i c_{ij} \quad (2)$$

Initial and Boundary conditions

$$c_{ij+1}(z, 0) = c_{ij}(z, t^*); \quad c_{i1}(z, 0) = c_{iNC}(z, t^*) \quad (3)$$

$$c_{ij}|_{z=0^-} = c_{ij}|_{z=0^+} - \frac{D_i}{v_j L} \frac{\partial c_{ij}}{\partial z} \Big|_{z=0^+}; \quad \frac{\partial c_{ij}}{\partial z} \Big|_{z=L} = 0 \quad (4)$$

Node Balances

$$Q_1 = Q_4 + Q_D; \quad c_{i1}^{in} Q_1 = c_{i4}^{out} Q_4 \quad (5)$$

$$Q_2 = Q_1 - Q_E; \quad c_{i2}^{in} = c_{i1}^{out} = c_i^E \quad (6)$$

$$Q_3 = Q_2 + Q_F; \quad c_{i3}^{in} Q_3 = c_{i2}^{out} Q_2 + c_i^F Q_F \quad (7)$$

$$Q_4 = Q_3 - Q_R; \quad c_{i4}^{in} = c_{i3}^{out} = c_i^R \quad (8)$$

Next, appropriately defined dimensionless variables are introduced (see Rajendran et al. 2009 for details). Note that since the states are multiplied by flow rates in Eqs. 5-8, the PDE represents a nonlinear model.

Glucose-fructose separation is considered as a test bed to study multiple modeling approach of SMBC that corresponds to an experimental setup of 1-1-1-1 column configuration as shown in Fig. 1, yielding  $NC = 4$  and  $n_c = 2$ . Separation takes place on a strongly acid cationic resin of gel type ( $Ca^{2+}$  form) on which fructose gets preferentially adsorbed relative to glucose. Deionized water is used as the desorbent. Fructose rich stream is drawn out as extract, which is considered as the main product. Model parameters corresponding to the SMBC and the glucose/fructose separation are summarized in Table 1. We use the method of orthogonal collocation on finite elements (OCFE) with roots of the shifted legendre polynomial for discretization of spatial finite elements to solve the PDE's in Eqs. (1)-(4) (Toumi et al., 2007). The spatial domain is discretized with 12 finite elements per column and 5 internal collocation point per finite element. This results in a total of 1160 states. This was found to be appropriate by comparing with several discretization schemes to obtain a set of ODEs of the form of Eq. (9) which is assumed as plant. The model equations were solved using ode 23 in MATLAB (R2007) on an Intel i7 machine.

Table 1. Parameters for Glucose/Fructose Separation

Parameter	Values	Parameter	Values
$d_c$ (cm)	2.54	$k$ ( $s^{-1}$ )	0.1
$L$ (cm)	40	$\epsilon$	0.4
$K_{fru}$	0.5634	$n_c$	2
$K_{glu}$	0.3401	$c_{glu}^F, c_{fru}^F$ (g/l)	30

### 3. MULTIPLE MODELING OF SMBC: A BAYESIAN APPROACH

This section deals with multiple model representation of the SMBC given in Section 2. The following steps are performed to obtain a global multiple model.

- (1) Generation of control relevant models,
- (2) Generation of "brother models" to account for the four switching configurations of SMB,
- (3) Aggregation of multiple linear models.

#### 3.1 Generation of control relevant models

Eqs. (1)-(8) represent an index-1 PDAE model of SMBC which performs the role of the true plant in this study. A corresponding ODE-IVP is obtained by method of lines, wherein only the spatial dimension is discretized using OCFE (Toumi et al., 2007). This yields the following form:

$$\mathcal{M}\dot{\mathbf{x}} = f(\mathbf{x}, \mathbf{u}) \quad (9)$$

where,  $\mathbf{x} \in \mathbb{R}^n$  represents the state vector,  $\mathbf{u} \in \mathbb{R}^m$  represents the input vector, and  $\mathcal{M} \in \mathbb{R}^{n \times n}$  is the mass matrix. The state vector  $\mathbf{x}$  includes the concentrations at each collocation point for four columns of the SMBC. Let  $c_A, c_B$  denote concentration of glucose and fructose in liquid phase, respectively and let  $q_A, q_B$  denote their respective concentrations in solid phase. Then the state vector is represented by,

$$\mathbf{x} = [c_A^1 T \dots c_A^4 T \quad c_B^1 T \dots c_B^4 T \quad q_A^1 T \dots q_A^4 T \quad q_B^1 T \dots q_B^4 T]^T \quad (10)$$

where  $c_A^1, c_B^1, q_A^1, q_B^1$  represent spatially distributed concentration vectors in liquid and solid phases for respective components for the first column of SMBC and similarly for other columns. The input vector  $\mathbf{u} = [Q_1, \dots, Q_4]^T$  represents internal flow rates corresponding to the four columns. In this study, a known constant switch time ( $t$ ) is assumed. To obtain multiple linear modes, the continuous time nonlinear model Eq. (9) is transformed to a set of linear models by Taylor series approximation at different operating points. Let  $\mathbf{M}^i$  represent the  $i^{th}$  linear model of the same order, obtained by linearizing at  $(\mathbf{x}_s^i, \mathbf{u}_s^i)$  and  $N_m$  be total number of linear models generated. Then the linear model  $\mathbf{M}^i$  evaluated at  $(\mathbf{x}_s^i, \mathbf{u}_s^i)$  takes the form,

$$\mathcal{M}\dot{\mathbf{x}} = f(\mathbf{x}_s^i, \mathbf{u}_s^i) + A^i \Delta \mathbf{x} + B^i \Delta \mathbf{u} \quad (11)$$

where,  $\Delta \mathbf{x} = (\mathbf{x} - \mathbf{x}_s^i)$ ,  $\Delta \mathbf{u} = (\mathbf{u} - \mathbf{u}_s^i)$   $A^i \in \mathbb{R}^{n \times n}$ ,  $B^i \in \mathbb{R}^{n \times m}$  are Jacobian matrices with respect to state vector ( $\mathbf{x}$ ) and input vector ( $\mathbf{u}$ ) respectively and  $f(\cdot)$  is the affine term. Since, the CSS points of SMBC operation do not correspond to actual steady state equilibrium points of Eq.(9), the affine term  $f(\cdot)$  encountered in Eq. (11) along CSS trajectory poses problems in terms of requirement for large number of multiple models to track the operating trajectory accurately. Hence, we choose equilibrium points obtained without port switching and not states along the CSS. This ensures that the multiple models are linear without the affine term. Since each of these models do not incorporate the effect of switching, we need to generate linear models that account for the switching. These sub-models are referred to as "brother models" and discussed next.

### 3.2 Generation of “brother models” to account for switching

The configurations of SMB due to switching need adequate care while obtaining multiple models. The initial configuration corresponding to mode 1 is shown in Fig. 1, with the feed entering between Sections 2 and 3. For an SMBC with four columns, there would be four switching modes. For mode 1, linearization around the CSS is performed to obtain linear models. Let  $\mathbf{x}_s^1 = [c_A^1 c_A^2 c_A^3 c_A^4 c_B^1 c_B^2 c_B^3 c_B^4 q_A^1 q_A^2 q_A^3 q_A^4 q_B^1 q_B^2 q_B^3 q_B^4]^T$  and  $\mathbf{u}_s^1 = [Q_1 Q_2 Q_3 Q_4]^T$  represent the steady state vectors for state and input for mode 1, respectively. A unique steady state input and state vector results from solving the true plant model corresponding to a specific performance objective as performed in Vignesh et al. Since switching resets states, the steady-state vectors for mode 2 is computed as  $\mathbf{x}_s^2 = [c_A^2 c_A^1 c_A^2 c_A^3 c_B^1 c_B^2 c_B^3 c_B^4 q_A^1 q_A^2 q_A^3 q_A^4 q_B^1 q_B^2 q_B^3 q_B^4]^T$ ,  $\mathbf{u}_s^2 = [Q_4 Q_1 Q_2 Q_3]^T$  and are similarly computed for the other modes as well. The SMB model Eqs. (1)-(8) are further linearized at these steady-states to obtain a bank of models as shown in Fig. 2. This completes a cycle of SMB operation and the result is a set of four “brother models” (due to four columns here) for each model  $\mathbf{M}_i$  generated at equilibrium point, which forms the basis for future prediction of SMB plant. Let  $\mathbf{M}^i$  model's  $j^{\text{th}}$  “brother model”  $\mathbf{M}_j^i$  dynamics be represented by,

$$\mathcal{M}\mathbf{x}_j^i = A_j^i \Delta \mathbf{x}_j^i + B_j^i \Delta \mathbf{u}, j \in S = \{1, 2, 3, 4\} \quad (12)$$

Let  $\sigma(t)$  be an indicator function,

$$\mathbb{R}_+ \rightarrow S : \sigma(t) = j \quad (13)$$

which identifies the switching mode of SMBC. Then,  $\mathbf{M}^i$  model dynamics considering the “brother models” corresponding to the four switching modes of the SMBC can be represented as

$$\mathcal{M}\mathbf{x}^i = A_{\sigma(t)}^i \Delta \mathbf{x}^i + B_{\sigma(t)}^i \Delta \mathbf{u} \quad (14)$$

“Brother models” (see Fig. 2) represent a model corresponding to a single equilibrium point  $(\mathbf{x}_s^i, \mathbf{u}_s^i)$  that is shifted in accordance with the switching modes of SMB operation, namely,  $\{1, 2, 3, 4\}$  respectively. These “brother models” are distinguished by rearranged entries of Jacobian matrices corresponding to these shifted steady-state vectors. However, in this work all the “brother models” generated from an equilibrium point are considered as part of a single model. The same process is repeated for a new equilibrium point to obtain a new set of “brother models”.

### 3.3 Aggregation of multiple linear models using Bayesian strategy

In conventional Bayesian weighting strategy, error between true plant and one-step ahead predictions of multiple models are used to generate the weights for aggregation. The aggregated multiple model is then used for long range predictions. But for systems which exhibit periodic evolution in state dynamics, weights obtained using one-step ahead predictions do not necessarily manifest in good long range predictions. Hence, for SMB, a system which exhibits periodic dynamics, a thorough analysis of the periodicity should be considered in order to design a successful weighting strategy. It was observed that at CSS,

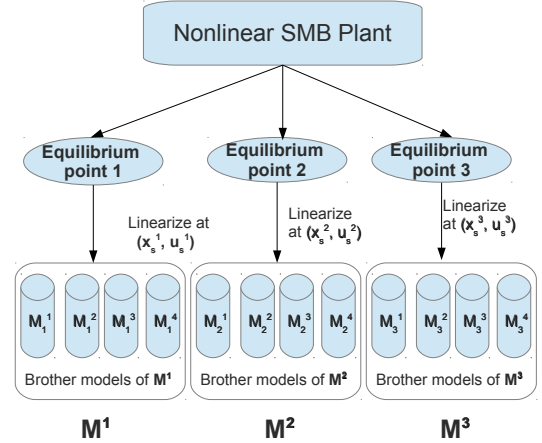


Fig. 2. Multiple models generation by linearization

the state (concentration) profiles repeat themselves in a one-period regime as shown in Fig. 3 with a period  $p$ . Hence we propose the notion of Bayesian weighting based on one-period prediction and use one-period prior state information,  $\mathbf{x}(k-p)$ , with reference to the current state information,  $\mathbf{x}(k)$ , as initial condition in order to predict one-period ahead state,  $\mathbf{x}(k+p)$ .

In the absence of full state measurement, an observer based aggregation of multiple models using Bayesian strategy to evaluate the weighted model is illustrated in Fig. 4. The approach integrates two Bayesian weight calculations each with specific functionalities:

*Bayesian weight calculator 1:* To predict  $\hat{\mathbf{x}}(k-p|k-p-1)$ , in order to estimate complete states from  $k-p+1, \dots, k$  leading to prior period profile, the steps are indicated below:

- Individually simulate the linear models  $\mathbf{M}_i$  one-step ahead;  $i = 1, \dots, N_m$
- Compute the innovation vector for each model  $\mathbf{M}_i$  using plant measurement at  $k-p$ , as

$$e_i(k-p) = \mathbf{y}(k-p) - \hat{\mathbf{y}}_i(k-p|k-p-1) \quad (15)$$

- Compute the posterior probability of the  $i^{\text{th}}$  linear model  $\mathbf{M}^i$  which is calculated as follows (Nandola and Bhartiya, 2008),

$$\mathbf{P}_{ri,k-p}(e) = \frac{\exp(-\frac{1}{2}e_{i,k-p}^T \mathbf{K} e_{i,k-p}) \mathbf{P}_{ri,k-p-1}(e)}{\sum_{j=1}^{N_m} \exp(-\frac{1}{2}e_{j,k-p}^T \mathbf{K} e_{j,k-p}) \mathbf{P}_{rj,k-p-1}(e)} \quad (16)$$

where  $\mathbf{P}_{ri,k-p-1}(e)$  is the prior probability

- Calculate the weights  $w_i$  corresponding to each model  $\mathbf{M}_i$  given by,

$$w_{i,k-p} = \frac{\mathbf{P}_{ri,k-p}(e)}{\sum_{l=1}^{N_m} \mathbf{P}_{rl,k-p}(e)} \quad (17)$$

- Then the estimated state at  $k-p$  is obtained as:  $\hat{\mathbf{x}}(k-p|k-p-1) = \sum_{i=1}^{N_m} w_{i,k-p} \hat{\mathbf{x}}_i(k-p|k-p-1)$ . The states corresponding to the measurements are updated directly.

*Bayesian weight calculator 2:* To predict one-period ahead  $\hat{\mathbf{x}}(k+p|k)$  from the current state  $\hat{\mathbf{x}}(k|k-p)$  (refer Fig. 3), the steps are indicated below:

- Obtain  $\hat{\mathbf{x}}_i(k|k-p)$  by simulating the models individually using estimated states ( $\hat{\mathbf{x}}(k-p|k-p-1)$ ) from Bayesian weight calculator 1
- Compute the innovation vector for each model  $\mathbf{M}_i$  using plant measurement at  $k$ , as

$$E_i(k) = \mathbf{y}(k) - \hat{\mathbf{y}}_i(k|k-p) \quad (18)$$

- Compute the posterior probability  $\mathbf{P}_{ri,k}(E)$  using the Eq. (16) and weights  $W_{i,k}$  using Eq. (17)
- Obtain the global model for the  $k^{th}$  instant by,

$$\mathbf{M}_k^{global} = \sum_{i=1}^{N_m} (W_{i,k}) \mathbf{M}^i, \text{ where } i = 1, \dots, N_m \quad (19)$$

$\mathbf{M}_k^{global}$  provides one-period ahead prediction.

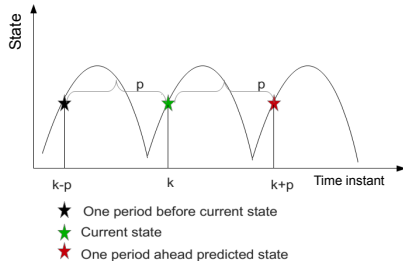


Fig. 3. One period ahead prediction

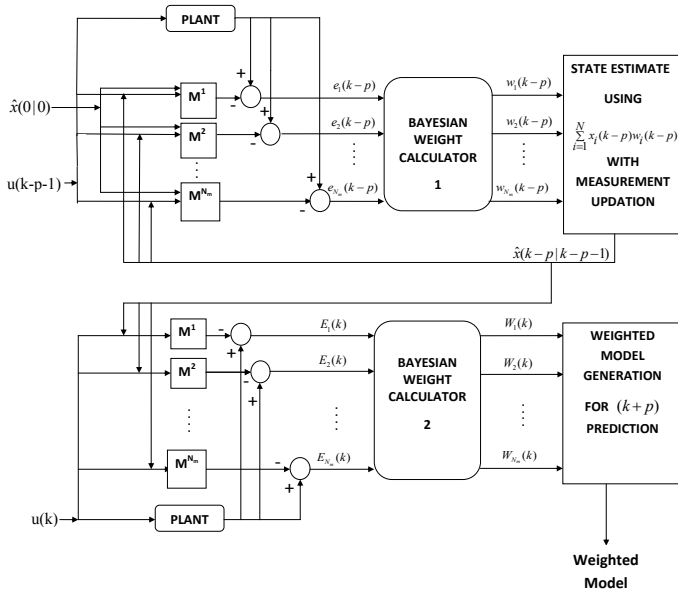


Fig. 4. Bayesian weighting with multiple models

$\mathbf{K}$  is a diagonal matrix and acts as a tuning parameter. In light of Bayes' rule,  $\mathbf{K}$  can be interpreted as the covariance of the likelihood and is typically chosen to be diagonal. Thus, higher the values of the elements of  $\mathbf{K}$ , the rejection of models with larger residuals is more likely. The user-defined  $\mathbf{K}$  allows strategies ranging from a winner-take-all approach (large  $\mathbf{K}$ ) to a non-discriminating averaging approach (small  $\mathbf{K}$ ).

In Bayesian aggregation, the weights of poorly performing models are small but not zero, thereby contributing to the overall model composition. This "excessive" competition from "unnecessary" models deteriorates the composite

model performance, which motivates using a parsimonious set of models.

#### 4. SIMULATION RESULTS

In this section, we validate the performance of the multiple models presented in Section 3 based on its (1) cyclic steady state performance (2) performance during transition operation from maximum purity to maximum throughput.

##### 4.1 CSS Performance: multiple model validation

Several researchers have presented the optimal CSS operation of SMBC (Zhang et al., 2002; Kawajiri and Biegler, 2006). Here we report validation of multiple models performance using the optimal CSS profile for three different fundamental goals:

- **Maximum throughput at CSS:** Referring to Fig. 1, throughput is defined as

$$Q_F = Q_3 - Q_2 \quad (20)$$

- **Maximum average extract purity at CSS:** In the maximal fructose purity mode of operation, the purity of fructose in the extract averaged over a switch period is maximised.

$$Pur_{Ex} = \frac{\int_0^{t^*} c_{Fr,u,Ex}(t) dt}{\int_0^{t^*} c_{Glu,Ex}(t) dt + \int_0^{t^*} c_{Fr,u,Ex}(t) dt} \quad (21)$$

Table 2. Optimal internal flow rates obtained from CSS optimization case studies

Parameter (ml/min)	Maximum throughput	Maximum Purity	Maximum Recovery
$Q_1$	43.23	43.23	43.23
$Q_2$	32.89	35	33.90
$Q_3$	37.17	36	34.90
$Q_4$	29.34	28.73	30.03

Table 2 presents the optimal solution for the above 3 cases using the simultaneous approach for optimization presented in Kawajiri and Biegler (2006) and Toumi et al. (2007). For further details regarding the cyclic steady state optimization problem formulation and results, the reader is referred to Vignesh et al.. The results of the optimization problem form the basis for performance validation of multiple models at CSS operation.

The weighted multiple model as discussed in Section 3 is used to predict three operational modes corresponding to: Maximum throughput at CSS and Maximum extract purity at CSS. Here, we assume that full-state information pertaining to 1160 true plant states are available. The one-period ahead predictions based on the three linear models individually and the estimation error ( $E_i$ ) are computed by comparing the true plant and predicted state information. Calculated error ( $E_i$ ) with respect to individual model prediction is fed to Bayesian weight calculator to find the weighted model. This weighted model is used to predict 1-period ahead, which in turn corresponds to 10-step ahead prediction as the step size is 0.1 times the normalized time.

The errors and weights calculated at time instant  $k$  are used to evaluate weighted model to perform prediction at  $(k + 10)^{th}$  time instant. These results are shown in Fig. 5, where Fig. 5a, 5b and 5c represent CSS corresponding to maximum throughput, maximum purity and maximum recovery, respectively. It can be seen from Fig. 5 that in each steady state, one linear model behaves very well, but other models perform poorly indicating that a multiple model would perform adequately in all three cases. Thus, a weighted multiple model based on the error from different models can represent the SMB operation globally.

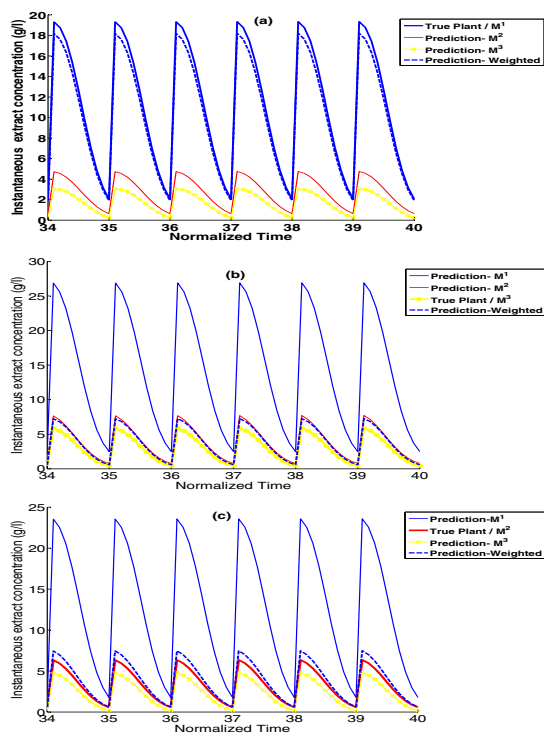


Fig. 5. Multiple modeling performance validation

#### 4.2 Optimal transition between maximum purity CSS to maximum throughput CSS: Multiple model performance validation

For flexible operation of SMB, it is imperative that the same process unit be able to satisfy varied performance objectives. This necessitates transiting from one optimal operating point to another. The transition that we consider here is from maximum purity CSS to maximum throughput CSS. This transition is analogous to servo control, where the objective is to steer the plant from one operating point to another. In this regard, we validate the quantitative performance of multiple model approach to be viable for applications that need long range predictions such as MPC.

Fig. 6 shows the comparison of multiple model performance with evolution of true plant instantaneous extract concentration (measured variable). During this transition case study, we assume that only outlet extract and raffinate concentrations (refer to Fig. 1) are measured, which corresponds to only 4 out of 1160 states. The observer initial condition for Bayesian weight calculator 1 (refer to Fig. 4) is given as a 5% perturbation of the true plant

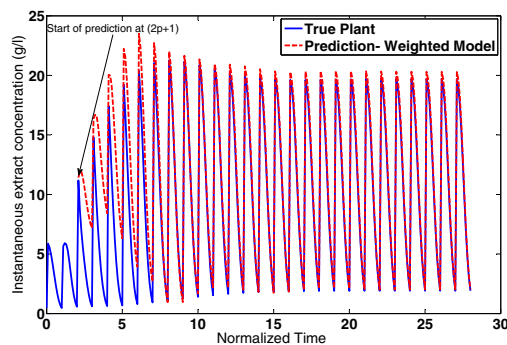


Fig. 6. Multiple modeling performance validation of measured state: extract concentration

initial condition. Bayesian weight calculator 1 provides the initial condition update ( $\hat{x}(k - p|k - p - 1)$ ) for Bayesian weight calculator 2 which in turn provides the weights ( $W_i$ ) for aggregating the single models. Therefore, the prediction using the weighted multiple model starts from  $(2p + 1)$  normalized time instant as indicated in Fig. 6. Initially, the response of the aggregated multiple model is not in complete agreement with plant dynamics for a measured state due to initial condition-mismatch. Subsequently, the plant measurement refines the observer states and the multiple model dynamics come in close agreement with true plant transition dynamics. Another reason for this discrepancy is attributed to the time needed for the prediction to capture the rapidly evolving state dynamics.

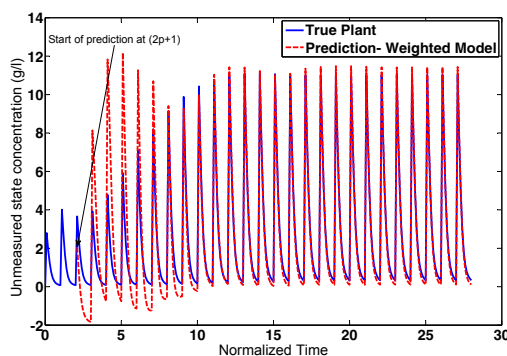


Fig. 7. Multiple modeling performance validation of unmeasured state ( $323^{rd}$  state of total 1160 states)

In addition, we validate the prediction capability of an unmeasured state using the aggregated multiple models and represent it in Fig. 7. It can be seen that the aggregated multiple model is able to predict closely its true state dynamics, after an initial offset. To show the superior performance of the aggregated multiple model with single models, 2-Norm prediction error is computed and plotted in Fig. 9. It can be seen that aggregated multiple model error decreases as the dynamics transit from a maximum purity CSS to a maximum throughput CSS. The error of the aggregated multiple model closely follows the best single model prediction at any given instant and an important point to be observed is the adaptation of the multiple model to align itself with the new CSS (maximum throughput CSS), that can be seen from Fig. 9 around normalized time = 11. The input profile for the transition study adopted for simulation is shown in Fig. 8. To quan-

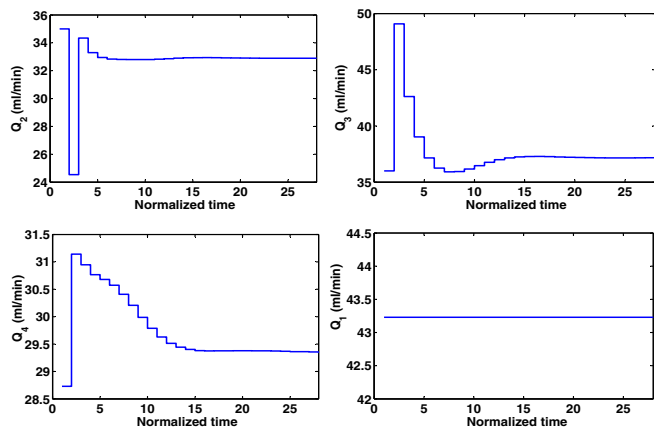


Fig. 8. Optimal Transition Inputs used for validation to identify the performance of the multiple model, we report the RMSE computed for the entire state dimension.

Table 3. RMSE for 1-period ahead prediction

Model	Model 1	Model 2	Model 3	Weighted model		
				$K = 10I_4$	$K = 25I_4$	$K = 50I_4$
RMSE	75.71	82.45	94.95	68.80	69.01	69.16

Table 3 reports performance of multiple models for different values of  $K$ . It was observed that with  $K = 10I_4$ , the aggregated weighted model converged to the least RMSE value as compared to individual linear models.

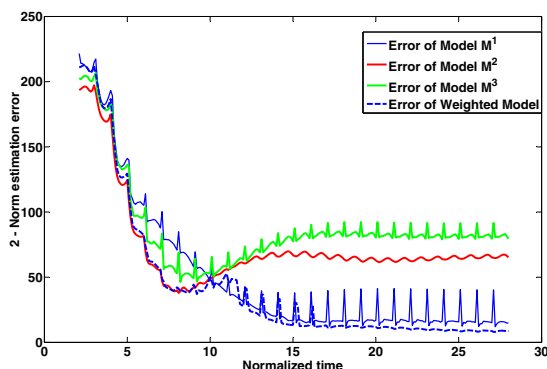


Fig. 9. Error comparison for single versus multiple models

## 5. CONCLUSIONS

In this work, we propose a multiple model approach as a control relevant model for SMBC. A key challenge was to address the switching nature of SMBC in the multiple linear models strategy. The simulation results confirm the superior performance of multiple model approach over single linear models. Such an approach will prove amenable for implementing Model Predictive Control (MPC) for faster online computation.

## 6. ACKNOWLEDGEMENT

The authors gratefully acknowledge funding from the Department of Science and Technology, India, under Grant number, 13DST057.

## REFERENCES

- M Alamir, F Ibrahim, and JP Corriou. A flexible nonlinear model predictive control scheme for quality/performance handling in nonlinear smb chromatography. *Journal of Process Control*, 16(4):333–344, 2006.
- A Banerjee, Y Arkun, B Ogunnaike, and R Pearson. Estimation of nonlinear systems using linear multiple models. *AIChE Journal*, 43(5):1204–1226, 1997.
- J Du and TA Johansen. A gap metric based weighting method for multimodel predictive control of mimo nonlinear systems. *Journal of Process Control*, 24(9):1346–1357, 2014.
- Gültekin Erdem, S Abel, M Morari, Marco Mazzotti, M Morbidelli, and JH Lee. Automatic control of simulated moving beds. *Industrial & engineering chemistry research*, 43(2):405–421, 2004.
- K Hariprasad, S Bhartiya, and RD Gudi. A gap metric based multiple model approach for nonlinear switched systems. *Journal of Process Control*, 22(9):1743–1754, 2012.
- Y Kawajiri and LT Biegler. Optimization strategies for simulated moving bed and PowerFeed processes. *AIChE Journal*, 52(4):1343–1350, 2006.
- K Klatt, F Hanisch, and G Dunnebieer. Model-based control of a simulated moving bed chromatographic process for the separation of fructose and glucose. *Journal of Process Control*, 12(2):203–219, February 2002.
- R Murray-Smith and TA Johansen. *Multiple model approaches to nonlinear modeling and control*. Taylor & Francis, London, UK, 1997.
- N Nandola and S Bhartiya. A multiple model approach for predictive control of nonlinear hybrid systems. *Journal of Process Control*, 18(2):131–148, 2008.
- S Natarajan and JH Lee. Repetitive model predictive control applied to a simulated moving bed chromatography system. *Computers & Chemical Engineering*, 24(2):1127–1133, 2000.
- A Rajendran, G Paredes, and M Mazzotti. Simulated moving bed chromatography for the separation of enantiomers. *Journal of Chromatography A*, 1216(4):709–738, January 2009.
- IH Song, SB Lee, HK Rhee, and M Mazzotti. Identification and predictive control of a simulated moving bed process: Purity control. *Chemical engineering science*, 61(6):1973–1986, 2006.
- A. Toumi, S. Engell, M. Diehl, H.G. Bock, and J. Schlder. Efficient optimization of simulated moving bed processes. *Chemical Engineering and Processing: Process Intensification*, 46(11):1067–1084, November 2007.
- SV Vignesh, Hariprasad K, P Athawale, S Vinod, and S Bhartiya. Optimal transition strategies for simulated moving bed chromatography. *Industrial & engineering chemistry research*, (In review).
- Z. Zhang, K. Hidajat, A. K. Ray, and M. Morbidelli. Multiobjective optimization of SMB and varicol process for chiral separation. *AIChE Journal*, 48(12):2800–2816, 2002.